

# Quantification of fingertip force reduction in the forefinger following simulated paralysis of extensor and intrinsic muscles

Francisco J. Valero-Cuevas<sup>a,b,\*</sup>, Joseph D. Towles<sup>a,c</sup>, Vincent R. Hentz<sup>a,d</sup>

<sup>a</sup>Rehabilitation Research and Development Center, Veterans Affairs Palo Alto Health Care System, Palo Alto, CA, USA

<sup>b</sup>Neuromuscular Biomechanics Laboratory, Sibley School of Mechanical and Aerospace Engineering, Cornell University, Ithaca, NY, USA

<sup>c</sup>Biomechanical Engineering Division, Mechanical Engineering Department, Stanford University, Stanford, CA, USA

<sup>d</sup>Hand Surgery Division, Department of Functional Restoration, Stanford University, Stanford, CA, USA

Accepted 30 May 2000

## Abstract

Objective estimates of fingertip force reduction following peripheral nerve injuries would assist clinicians in setting realistic expectations for rehabilitating strength of grasp. We quantified the reduction in fingertip force that can be biomechanically attributed to paralysis of the groups of muscles associated with low radial and ulnar palsies. We mounted 11 fresh cadaveric hands (5 right, 6 left) on a frame, placed their forefingers in a functional posture (neutral abduction, 45° of flexion at the metacarpophalangeal and proximal interphalangeal joints, and 10° at the distal interphalangeal joint) and pinned the distal phalanx to a six-axis dynamometer. We pulled on individual tendons with tensions up to 25% of maximal isometric force of their associated muscle and measured fingertip force and torque output. Based on these measurements, we predicted the optimal combination of tendon tensions that maximized palmar force (analogous to tip pinch force, directed perpendicularly from the midpoint of the distal phalanx, in the plane of finger flexion–extension) for three cases: non-paretic (all muscles of forefinger available), low radial palsy (extrinsic extensor muscles unavailable) and low ulnar palsy (intrinsic muscles unavailable). We then applied these combinations of tension to the cadaveric tendons and measured fingertip output. Measured palmar forces were within 2% and 5° of the predicted magnitude and direction, respectively, suggesting tendon tensions superimpose linearly in spite of the complexity of the extensor mechanism. Maximal palmar forces for ulnar and radial palsies were 43 and 85% of non-paretic magnitude, respectively ( $p < 0.05$ ). Thus, the reduction in tip pinch strength seen clinically in low radial palsy may be partly due to loss of the biomechanical contribution of forefinger extrinsic extensor muscles to palmar force. Fingertip forces in low ulnar palsy were 9° further from the desired palmar direction than the non-paretic or low radial palsy cases ( $p < 0.05$ ). © 2000 Elsevier Science Ltd. All rights reserved.

**Keywords:** Hand; Finger; Cadaveric; Muscle coordination; Low radial palsy; Low ulnar palsy; Paretic finger; Finger strength

## 1. Introduction

Weak tip pinch is an important clinical consequence of injury to the ulnar or radial nerves (Tubiana, 1981; Brand

and Hollister, 1993). Tip pinch, produced by opposing thumb and forefinger pulps, is weakened by the reduction in forefinger forces due to the paralysis of all finger and wrist extensor muscles (designated “low radial nerve palsy” in this paper) or intrinsic finger muscles (designated “low ulnar nerve palsy” in this paper) in these common injuries. Objective biomechanical estimates of finger force reduction directly attributable to these paralyzes would provide realistic predictions of the functional outcomes for these injuries.

Tip pinch weakness following low radial palsy is not well understood and is thought to be the consequence of wrist instability arising from paralysis of wrist extensor muscles. A common explanation holds that individuals with low radial palsy cannot forcefully maintain an extended wrist against the innervated extrinsic finger flexor

\* Correspondence address. Neuromuscular Biomechanics Laboratory, Sibley School of Mechanical and Aerospace Engineering, Cornell University 222 Upson Hall, Ithaca, NY 14853-7501, USA. Tel.: +1-605-255-3575; fax: +1-605-255-1222.

E-mail address: fv24@cornell.edu, <http://www.mae.cornell.edu/valero> (F.J. Valero-Cuevas).

Abbreviations: DI, first dorsal interosseous muscle; DIP, distal interphalangeal joint; EC, extensor digitorum communis muscle slip; EI, extensor indicis proprius muscle; EMG, electromyographic recordings; FP, flexor digitorum profundus muscle slip; FS, flexor digitorum superficialis muscle slip; LUM, first lumbrical muscle; MCP, metacarpophalangeal joint; PI, first palmar interosseous muscle; PIP, proximal interphalangeal joint; SD, standard deviation.

muscles, thus flexor muscles are involuntarily prevented from producing maximal force to maintain wrist stability (Bunnell, 1948; Brand and Hollister, 1993). However, paralysis of forefinger extensor muscles alone may reduce tip pinch force as evidenced by extensor activity predicted by a biomechanical model (Valero-Cuevas et al., 1998) and seen in electromyograms (EMG) of tip pinch (Close and Kidd, 1969; Long et al., 1970) and isometric fingertip forces (Valero-Cuevas et al., 1998; Valero-Cuevas, 2000). Low ulnar palsy, in contrast, does not affect wrist musculature, and tip pinch weakness is attributed to the paralysis of the intrinsic muscles of the fingers known to be active during tip pinch (Tubiana, 1981; Brand, 1990; Brand and Hollister, 1993).

There are no reliable estimates of the severity of force reduction in tip pinch following low radial and ulnar palsies. Clinical estimates of pinch strength in the paretic hand cannot distinguish between force reduction directly attributable to the paralysis of specific muscles, and weakness due to the secondary effects of paralysis on innervated musculature such as atrophy and need for re-education. Only one biomechanical model predicts force deficits in paretic fingers (Spoor, 1983), but our modeling and experimental work (Valero-Cuevas et al., 1998) has challenged its two-dimensional nature and simplification of the functional anatomy of the extensor mechanism.

Cadaveric preparations make no assumptions about digit anatomy but have not been used to study three-dimensional fingertip forces. Cadaveric studies have focused on the relationship between tendon pulley integrity and flexor tendon excursion (Mick et al., 1978; Hume et al., 1991; Rispler et al., 1996; Hamman et al., 1997; Nishida et al., 1998), or the transmission of flexor tendon tension to the fingertip (Greenwald et al., 1994; Rispler et al., 1996). However, no method has solved the muscle redundancy of the digits experimentally, or simultaneously applied tension to tendons to study the muscle coordination necessary to produce three-dimensional fingertip force.

Our first hypothesis is that paralysis of forefinger extensor muscles weakens fingertip force analogous to that used in tip pinch. We also hypothesize that paralysis of intrinsic finger muscles severely weakens that same fingertip force. These hypotheses were tested by applying mechanically optimal tension combinations to the appropriate tendons of cadaveric forefingers and measuring three-dimensional fingertip force.

## 2. Methods

In 11 thawed cadaveric arms (5 right, 6 left) resected at the mid-forearm level, we dissected the forefinger tendons of flexor digitorum profundus (FP), flexor digitorum superficialis (FS) and extensor digitorum communis (EC),

as well as extensor indicis proprius (EI) to tie and glue (Vetbond Tissue Adhesive, 3M Inc., St. Paul, MN) them to Nylon cords. The distal aponeuroses of first lumbrical (LUM) and first palmar interosseous (PI) were similarly attached to Nylon cords without dissecting their origins. The very short insertion tendon of first dorsal interosseous (DI) into the proximal phalanx of the forefinger (Tubiana, 1981; An et al., 1983; Ikebuchi et al., 1988; Brand and Hollister, 1993) precluded tying a cord to it. Instead, a Nylon cord was anchored to a 3-mm flathead screw placed at the insertion of DI into the proximal phalanx. The cadaver material used had been donated to the Division of Human Anatomy, Department of Surgery, Stanford University School of Medicine.

We mounted each cadaveric hand on a tabletop and fixed the distal phalanx to a six-axis dynamometer, programming the midpoint of the distal phalanx as the origin of force/torque measurement (Fig. 1). An external fixation device (Agee-WristJack, Hand Biomechanics Lab, Inc., Sacramento, CA) held the hand and forearm in neutral wrist extension and ulnar deviation. We placed the forefinger in a standardized posture of neutral abduction, 45° flexion at the metacarpophalangeal (MCP) and proximal interphalangeal (PIP) joints, and 10° flexion at the distal interphalangeal (DIP) joint. A robotic arm (Stäubli-Unimate Puma 260) allowed us to quickly and accurately move, and then rigidly hold, a six-axis dynamometer (F/T Gamma130, ATI Industrial Automation, Garner, NC) against the fingertip. Two K-wires protruding from the distal phalanx were clamped to the dynamometer. The 1.6-mm K-wires were inserted into the distal phalanx parallel to its longitudinal axis and were potted with polymethylmetacrylate (leaving the DIP joint and the insertions of the extensor mechanism and FP tendon intact). Pulling on and anchoring a thin rope tied to the proximal end of a spring was what stretched the spring. Because the springs were more compliant than the tendons, stretching the springs provided a constant tension within the 10% accuracy of the calibrated spring scale. The springs applied tensions up to 25% of the maximal strength of the muscle associated with each tendon. We applied the same tendon tensions to all specimens, which were derived from physiological cross-sectional areas (Jacobson et al., 1992; Lieber et al., 1992) and a biomechanical model (Valero-Cuevas et al., 1998) (Table 1). Because the forefinger was immobilized proximally and distally, applying tendon tensions did not affect finger posture.

We individually applied discrete levels of tension to each tendon (up to 25% of the maximal force of the muscle associated with each tendon) and recorded the six-dimensional fingertip output vector for each tendon tension level. To ensure only one tendon was loaded at a time, the Nylon strings of the tendons that were not receiving any load were disconnected from their associated springs. The output force and torque components

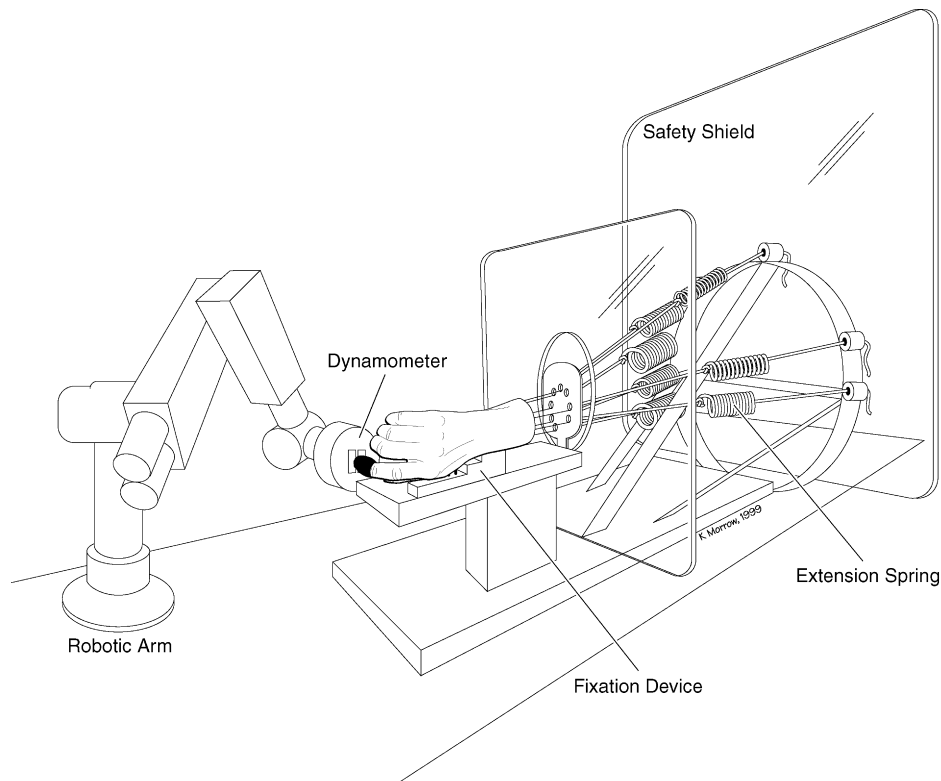


Fig. 1. Experimental apparatus. Fresh cadaveric hands were resected at the mid-forearm, rigidly mounted on a frame using an external fixation device and the insertion tendons of all forefinger muscles exposed. Nylon strings were glued to each insertion tendon, and the proximal end of each Nylon cord was fed proximally through radius-countersunk holes in a low-friction acetal resin (Delrin®, DuPont) plate before radiating out and attaching to the distal end of an extension spring. Hole locations set anatomically correct lines of action for the strings. Pulling on and anchoring a thin rope (Kevlar®, DuPont) tied to the proximal end of the spring was what stretched the spring and produced a constant tension at the tendon (read on a calibrated scale mounted with the spring,  $\pm 10\%$ ). Springs were chosen such that 0.20 m of extension produced 25% of the maximal isometric force. Preliminary tests established that tying and gluing string to tendon withstood up to 60 N, and the highest tension applied at the tendon of the strongest muscle (FS) was limited to 60 N (i.e., 25% of its maximal force; Valero-Cuevas et al., 1998). Because dorsal interosseous has a very short insertion tendon, its nylon string was tied to a 3-mm flathead screw placed at the insertion point of DI into the proximal phalanx. Two K-wires were potted into the distal phalanx with polymethylmethacrylate and rigidly clamped to a six-axis dynamometer rigidly held by a robotic arm. Known tensions could then be applied to individual tendons, and simultaneously to several tendons, and the fingertip force/torque output measured.

Table 1  
Correlation coefficient with tendon tension of each component of fingertip output and of fingertip force vector magnitude. Mean (SD);  $n = 11^a$

Tendon (max force, N)	Levels of tendon tension, % of maximal muscle force	Pearson product-moment correlation coefficients					Force vector magnitude
		$f_x$	$f_y$	$f_z$	$t_y$		
FP (120)	8.3, 12.5, 16.6, 20.8, 25	0.99 (0.009)	0.95 (0.045)	0.63 (0.25)	0.79 (0.21)	0.99 (0.009)	
FS (240)	4.1, 8.3, 12.5, 16.6, 20.8, 25	0.98 (0.013)	0.94 (0.03)	0.87 (0.096)	0.83 (0.21)	0.99 (0.012)	
EI (40)	12.5, 18.75, 25	0.82 (0.17)	0.83 (0.22)	0.93 (0.053)	0.7 (0.3)	0.95 (0.082)	
EC (100)	10, 15, 20, 25	0.79 (0.23)	0.63 (0.21)	0.93 (0.14)	0.79 (0.23)	0.98 (0.035)	
LUM (24)	8.3, 12.5, 16.6, 20.8, 25	0.85 (0.19)	0.82 (0.2)	0.97 (0.025)	0.56 (0.21)	0.96 (0.038)	
DI (120)	8.3, 12.5, 16.6, 20.8, 25	0.76 (0.25)	0.97 (0.05)	0.83 (0.2)	0.95 (0.048)	0.91 (0.13)	
PI (120)	8.3, 12.5, 16.6, 20.8, 25	0.82 (0.26)	0.90 (0.17)	0.98 (0.018)	0.96 (0.029)	0.98 (0.018)	

<sup>a</sup>Note that components of force more closely aligned with the muscle's resultant fingertip force (e.g.,  $f_x$  for FS tendon, Table 1, Figs. 2 and 3), by being least susceptible to measurement error, have higher correlation with tendon tension.

were measured with a resolution of 0.1 N and 0.01 N m, respectively. At each tendon tension level, a computer (PowerMacintosh 7200, Apple Computer, Inc., Cupertino, CA) with data acquisition hardware/software (NB-MIO-16 card and LabView, National Instruments, Aus-

tin, TX) recorded the output from the dynamometer for 2 s at 1000 S/s and stored the average fingertip output vector  ${}^6\mathbf{v} = \{f_x f_y f_z \tau_x \tau_y \tau_z\}^T$  produced by each tendon (subscript 6 denotes the number of elements in each vector; output forces are in units of N, torques in N m).

Linear programming (Chvátal, 1983) was used to predict the optimal combination of tendon tensions that produced the maximal magnitude of a desired resultant fingertip output vector  $\mathbf{b}$ . To simplify the optimization, and to be consistent with the kinematics of fingers that have one ad-abduction and three flexion–extension de-

The goal of linear programming in this study is to maximize force in the  $f_x$  (i.e., palmar) direction (perpendicular to the midpoint of the distal phalanx in the plane of finger flexion–extension, analogous to that used in pad-to-pad pinch, Fig. 2). The linear programming problem was stated as:

$$\begin{aligned} &\text{Find input tendon tension vector } \mathbf{u} \text{ to} \\ &\text{maximize the magnitude of } \mathbf{a}_{f_x}^T \mathbf{u} \\ &\text{subject to} \\ &- c_j \leq \mathbf{a}_j^T \mathbf{u} \leq c_j, \text{ where subscript } j \text{ denotes } f_y, f_z \text{ and } \tau_y \\ \\ &\mathbf{0} \leq \mathbf{u} \leq 25\% \mathbf{t}, \text{ where } 25\% \mathbf{t} = \left\{ 25\% t_{FP} \quad 25\% t_{FS} \quad 25\% t_{EI} \quad 25\% t_{EC} \quad 25\% t_{LUM} \quad 25\% t_{DI} \quad 25\% t_{PI} \right\}^T, \end{aligned}$$

grees-of-freedom (Yoshikawa, 1990; Valero-Cuevas et al., 1998), the  $\tau_x$  and  $\tau_z$  torque components were not considered. The fingertip output vector was defined as having four components: three-dimensional force plus a torque in the plane of finger flexion–extension,  $\tau_y$  (i.e.,  $\mathbf{b} = \{f_x \ f_y \ f_z \ \tau_y\}^T$ ). For each forefinger, we created a  $4 \times 7$  matrix  $\mathbf{A}$  whose column vectors  $\frac{25\%}{4} \mathbf{v}_i = \{f_x \ f_y \ f_z \ \tau_y\}^T$  consisted of 4 elements of the  $\frac{25\%}{4} \mathbf{v}$  vector recorded while producing 25% of maximal tension at tendon  $i$  (subscript 4 denotes the number of elements in the vector; superscript 25% denotes that it is the vector collected when 25% of maximal tension was applied). Each column of  $\mathbf{A}$  was normalized by dividing by the tension applied at its associated tendon.

where each  $c_j$  specifies the bounds on each of the undesired elements of  $\mathbf{b}$  with all positive tendon tensions  $\mathbf{u}$  bounded by  $25\% \mathbf{t}$  (25% of maximal muscle tensions, in units of N). The bounds  $c_j$  were chosen a priori to allow the three-dimensional output fingertip force to be deviated by at most  $15^\circ$  from the desired palmar direction, and the production of  $\tau_y$  to be less than 0.05 N m. Unexpectedly, as is shown in the results, simulating low ulnar palsy often resulted in the trivial solution when no coordination pattern could meet this  $15^\circ$  bound. In these cases, the directional constraint was relaxed  $1^\circ$  at a time until the first non-trivial solution was found. Linear programming algorithms in *Mathematica* mathematical package

$$\mathbf{A} = \begin{bmatrix} \frac{25\%}{4} \mathbf{v}_{FP} & \frac{25\%}{4} \mathbf{v}_{FS} & \frac{25\%}{4} \mathbf{v}_{EI} & \frac{25\%}{4} \mathbf{v}_{EC} & \frac{25\%}{4} \mathbf{v}_{LUM} & \frac{25\%}{4} \mathbf{v}_{DI} & \frac{25\%}{4} \mathbf{v}_{PI} \end{bmatrix}.$$

The matrix equation

$$\mathbf{A} \mathbf{u} = \mathbf{b} \tag{1}$$

calculates the resultant fingertip output vector  $\mathbf{b} = \{f_x \ f_y \ f_z \ \tau_y\}^T$  produced by an input vector of tendon tensions,  $\mathbf{u} = \{t_{FP} \ t_{FS} \ t_{EI} \ t_{EC} \ t_{LUM} \ t_{DI} \ t_{PI}\}^T$ . Tendon tensions are in units of N. The row vectors of matrix  $\mathbf{A}$  can be written as

$$\mathbf{A} = \begin{bmatrix} \mathbf{a}_{f_x}^T \\ \mathbf{a}_{f_y}^T \\ \mathbf{a}_{f_z}^T \\ \mathbf{a}_{\tau_y}^T \end{bmatrix},$$

where the  $i$ th row vector  $\mathbf{a}_i^T$  specifies the linear combination of the elements of  $\mathbf{u}$  that produces the  $i$ th element of the output vector  $\mathbf{b}$ . Then, Eq. (1) becomes

$$\begin{bmatrix} \mathbf{a}_{f_x}^T \\ \mathbf{a}_{f_y}^T \\ \mathbf{a}_{f_z}^T \\ \mathbf{a}_{\tau_y}^T \end{bmatrix} \mathbf{u} = \begin{Bmatrix} f_x \\ f_y \\ f_z \\ \tau_y \end{Bmatrix} \tag{2}$$

(Wolfram Research, Inc., Champaign, IL) were run on a minicomputer (DEC Alpha, Digital Equipment Corporation, Maynard, MA). In all specimens, the predicted optimal combinations of tendon tensions for maximal palmar force, which took a few minutes to calculate, were immediately implemented in the cadaver hand by

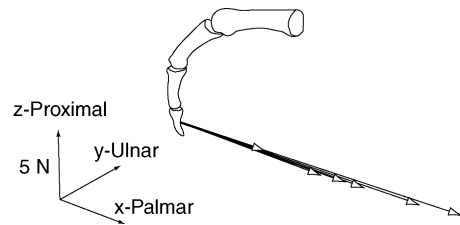


Fig. 2. Three-dimensional fingertip force output vectors recorded for different levels of tension at the FS tendon of one right-hand specimen (for clarity, output fingertip torque is not shown). The coordinate frame used to describe fingertip output is defined in the anatomical position and is fixed to the midpoint of the distal phalanx as the finger flexes into the standardized posture. The  $x$  direction represents the desired palmar force direction defined to be in a direction analogous to that used in pad-to-pad tip pinch, perpendicular to the distal phalanx and in the plane of finger flexion–extension.

applying the prescribed tensions at each tendon and measuring the resultant fingertip output vector.

Lastly, we predicted maximal palmar force for low radial and ulnar palsies for all specimens. The appropriate muscles were removed by replacing the appropriate columns of **A** with zero vectors. Namely, EI and EC columns were removed for the low radial palsy case, and LUM, DI and PI columns for the low ulnar palsy case. The optimal combinations of tendon tensions predicted for low ulnar and radial palsy cases were implemented experimentally in 11 and 5 specimens, respectively, by applying the prescribed tensions at each tendon and measuring the resultant fingertip output vector.

### 3. Results

Fingertip output,  $\mathbf{v}$ , scaled linearly with the magnitude of the input tension applied at each tendon (see Fig. 2

for an example). Table 1 lists the mean Pearson product-moment correlation coefficient of  $f_x, f_y, f_z, \tau_y$  output components and of fingertip force vector magnitudes with tendon tension. The mean fingertip force vector magnitude and direction for 25% of maximal tension at each tendon for all specimens are plotted in Fig. 3 (for an interactive exploration of all three-dimensional data see the webpage of the Journal of Biomechanics: <http://www.mae.cornell.edu/valero/JBiomech>

The mechanical effect of individual tendons superimposed linearly when tension was applied to multiple tendons simultaneously given that the measured fingertip output was equivalent to the vector sum of the fingertip outputs produced by individual tendons. Maximal palmar forces measured in the cadaveric fingers were not significantly different from those predicted by linear programming (Table 2). On average, measured fingertip force magnitudes were within 2% of their predicted value and were directed within 5° of their predicted direction.

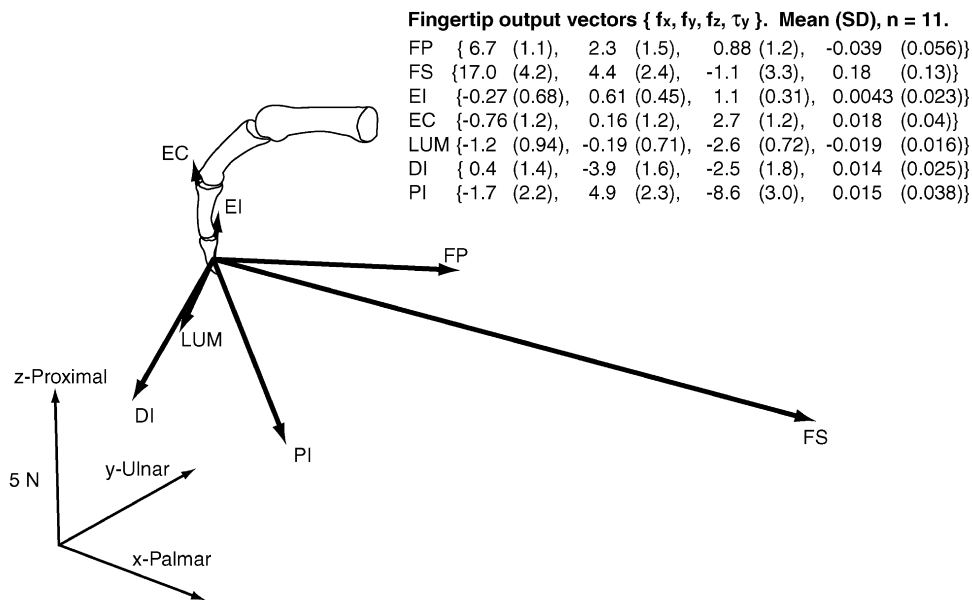


Fig. 3. Average maximal fingertip force output vector for 25% of maximal tension applied at each tendon (for clarity, output fingertip torque is not shown). Forces in N, output fingertip torque in Nm, mean (SD),  $n = 11$  (5 right and 6 left forefingers; data from left forefingers was appropriately rotated to a right forefinger orientation).

Table 2  
Comparison of predicted and measured fingertip forces. Mean (SD)<sup>a</sup>

	Non-paretic		Low ulnar palsy		Low radial palsy	
	Force	Angle	Force	Angle	Force	Angle
Predicted	1.0 (0)	10.51 (8.74)	0.44 (0.23)	16.99 (8.61)	0.84 (0.14)	10.81 (7.83)
Measured	1.02 (0.11)	10.40 (5.34)	0.43 (0.24)	21.9 (10.89)	0.86 (0.12)	8.23 (5.69)
Average	1.01 (0.08)	10.45 (7.06)	0.43 (0.22)*	19.48 (9.91)*	0.85 (0.13)*	9.95 (7.09)

<sup>a</sup>Force magnitudes are compared by normalizing to the magnitude of the maximal predicted palmar force in each specimen. The average maximal palmar force magnitude was 11.8 (4.1) N. The angles shown (in degrees) are the deviation from the target  $x$  direction in Fig. 2 (i.e., perpendicular to the distal phalanx in the plane of finger flexion–extension). Asterisks indicate a significant difference from non-paretic case (Analysis of variance and Tukey–Kramer post-hoc pairwise comparisons;  $p < 0.05$ ).

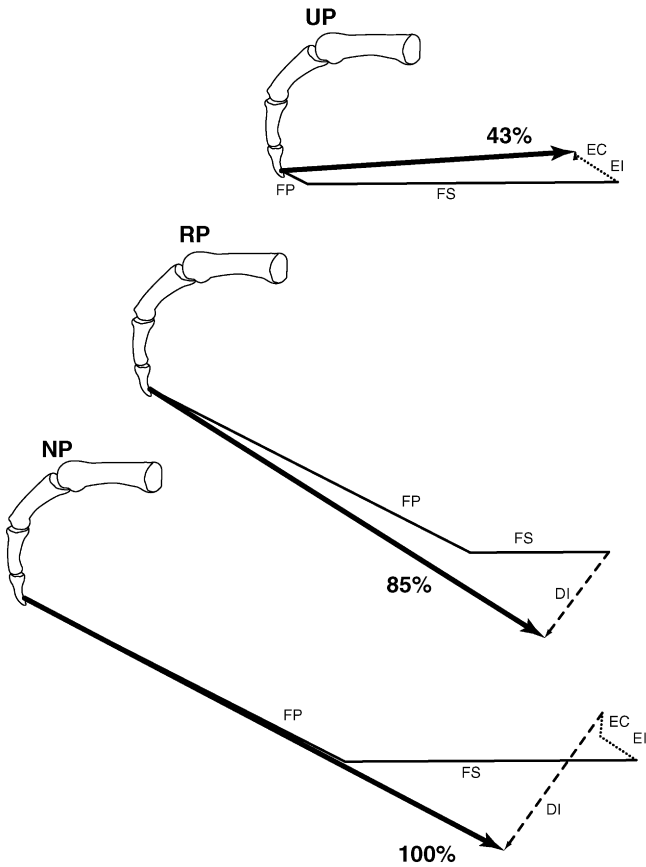


Fig. 4. Sample three-dimensional plot of the optimal vector addition of tendon actions that achieve maximal palmar force in the non-paretic (NP), low radial palsy (RP) and low ulnar palsy (UP) cases in one specimen. Percentages indicate magnitude relative to the NP case (Analysis of variance and Tukey–Kramer post-hoc pairwise comparisons;  $p < 0.05$ ). For clarity, fingertip output torque is not shown.

Simulating low radial and ulnar palsies resulted in significantly lower maximal palmar force magnitudes relative to the non-paretic cases (Table 2,  $p < 0.05$ ). The average maximal palmar force for the non-paretic case was 11.8 (4.1) N, which dropped by 15% when both extensors were unavailable, and by 57% when intrinsic muscles were removed. Fig. 4 shows example optimal predictions for one specimen in all cases.

Simulating low ulnar palsy resulted in significantly reduced tension at the tendons of extrinsic muscles ( $p < 0.05$ ). In contrast, simulating low radial palsy only resulted in non-significant reduction of both flexor and DI tendon tensions (see Fig. 5A). If those results are normalized by fingertip force magnitude, nearly similar results follow (see Fig. 5B).

Simulating low ulnar palsy reduced the accuracy with which fingertip force could be directed in the palmar direction relative to the other cases (Table 2,  $p < 0.05$ ). The simulated low ulnar palsy resulted in fingertip force being directed, on average, within 19° from the palmar direction, compared to approximately 10° for the other two cases (Table 2).

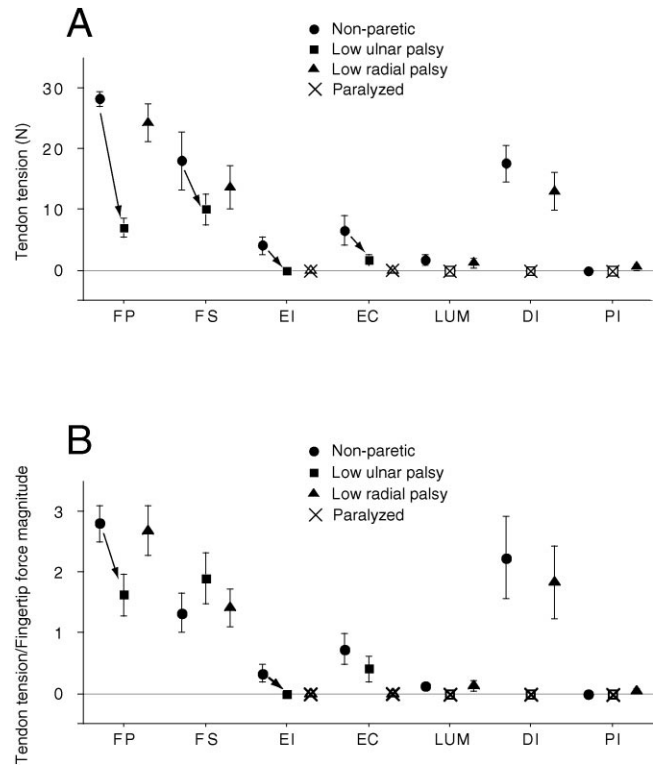


Fig. 5. (A) Mean tendon tension with standard error bars for maximal palmar force for all three cases and all specimens. (B) Mean ratio of tendon tension to fingertip force magnitude with standard error bars for all three cases shows similar results as in (A) with the exception of FS. The ratio of FS tension to fingertip force magnitude was statistically similar, but numerically higher, in both simulated palsies compared to the non-paretic case. Arrows indicate a statistically significant change from the non-paretic case (Analysis of variance and Tukey–Kramer post-hoc pairwise comparisons;  $p < 0.05$ ).

#### 4. Discussion

This study is unique in that it combines parameter optimization with an empirical mathematical model obtained from cadaver forefingers. We employ this novel approach to quantify the mechanically expected reduction of fingertip force following common peripheral nerve injuries. We essentially substituted the central nervous system control over the forefinger by a method that found and applied mechanically optimal tendon tensions to maximize palmar force. Importantly, this approach makes quantitative estimates of maximal palmar force without making assumptions about forefinger anatomy (e.g., moment arms).

The evidence of intra- and inter-tendon linearity demonstrates that tendon tensions scale and superimpose linearly when producing fingertip force — an assumption often made in classical biomechanical computer models (An et al., 1979; Spoor, 1983; Valero-Cuevas et al., 1998), but not previously validated experimentally. Intra-tendon linearity was evidenced by the high correlation of fingertip force magnitude with tendon tension in Table 1.

Inter-tendon linearity was demonstrated during the simultaneous application of tendon tensions by the fact that the magnitude and direction of the predicted and measured resultant fingertip force vectors were statistically similar. The linear scaling and superimposition of tendon actions is particularly interesting in the case of human digits. Our results suggest the complex interconnections (Tubiana, 1981; Zancolli and Cozzi, 1992) and viscoelastic material properties (Garcia-Elias et al., 1991; Hurlbut and Adams, 1995) of the extensor mechanism, as well as the complex relationship between LUM and FP, do not introduce significant non-linearities to transmission of tension of EI, EC, LUM, FP and PI tendons in the finger posture studied. These results, however, do not rule out non-linear changes in transmission of tendon tension with the known changes in the geometric arrangement of the extensor mechanism at different finger postures (Garcia-Elias et al., 1991).

The limitations of this cadaveric/numeric study include the exclusion of physiological secondary effects of paralysis (such as sensory deficit and muscle re-education), and the inability to predict the consequences of modifying a specific anatomical feature mathematically (as parameter-based computer models can (An et al., 1979; Spoor, 1983; Valero-Cuevas et al., 1998)). By representing individual anatomical features as mathematical parameters, classical biomechanical computer models can use sensitivity analysis to determine which anatomical features affect functional outcomes the most (An et al., 1979; Spoor, 1983; Valero-Cuevas et al., 1998). Furthermore, this study cannot evaluate the possible wrist instability due to paralysis of wrist extensor muscles in low radial palsy, although the methodology presented here can be extended to include wrist extensor muscles to address this issue. Also, although the  $\tau_x$  and  $\tau_z$  torque components of fingertip output were low in magnitude, future studies could explore their functional implications. The passive transfer of force between LUM and FP was not investigated here (they were assumed to be independent muscles). Lastly, recognizing that LUM of the forefinger may be innervated by the median or ulnar nerves, or at times both (Brand and Hollister, 1993), we chose to remove its action in low ulnar palsy to obtain a worst-case estimate of force reduction. The estimates of maximal palmar forces presented in this study are the biomechanical upper bound for worst-case, complete nerve injuries. Clinical pinch force reduction may be less severe than predicted here in cases of incomplete nerve injury, partial recovery of nerve function, or variable muscle innervation. In spite of these limitations, the predicted maximal non-paretic palmar force of 11.8 N with 25% of muscle strength is equivalent to 47.2 N at 100% strength — which falls within the reported range of maximal tip pinch forces (19–106 N; Weightman and Amis, 1982; An et al., 1985; Mathiowetz et al., 1985; Valero-Cuevas et al., 1998). Furthermore, the methodology presented here can

be used to study structural secondary effects of paralysis (e.g., tendon adhesions); improve functional outcomes by simulating and evaluating surgical procedures; and increase the impact of biomechanical computer models on clinical practice by corroborating their predictions.

The simulated paralysis of extrinsic extensor muscles of the forefinger suffices to reduce maximal biomechanically feasible palmar force magnitude, suggesting extensor muscles play a necessary biomechanical role to maximize palmar force. Fig. 5A shows that, without extrinsic extensor muscles, the mean tensions in FP, FS, LUM and DI are lower, although not statistically so, than the non-paretic case. This numerical reduction in tendon tension in four out of five active muscles leads to a significant 15% reduction in maximal palmar force. The biomechanical contribution of EI and EC can be seen geometrically in Figs. 3 and 4. By having a strong positive  $z$  (proximal) component, EI and EC cancel the negative  $z$  component of DI. Once the negative  $z$  contribution of DI is cancelled, the fingertip force of DI has mostly a negative  $y$  (radial) component that can counteract the positive  $y$  (ulnar) component of FP and FS. In this way, FP and FS can be active at higher levels to increase their component in the palmar direction without the net output fingertip force being unduly ulnarly deviated.

The paralysis of intrinsic muscles not only severely reduces the maximal biomechanically feasible palmar force magnitude, but also compromises the ability to properly direct fingertip force ( $p < 0.05$ ). Fig. 5A shows that, without intrinsic muscles, the mean tension in FP, FS, EI and EC is statistically lower than in the non-paretic case. This significant reduction in tendon tension in all non-paretic muscles leads to a severe 57% reduction in maximal palmar force. Geometrically, Figs. 3 and 4 again show that the absence of DI represents the loss of the only muscle with a strong negative  $y$  (radial) component, leaving the low ulnar palsy forefinger with the ability to produce ulnarly deviated fingertip forces only. Therefore, restoring the strong negative  $y$  (radial) action of DI in the forefinger — as opposed to the current practice of creating a central MCP flexor muscle (e.g., Zancolli Lasso: Brand and Hollister, 1993) — may be a more effective way to restore pinch strength and dexterity while preventing MCP hyper-extension deformity in patients with low ulnar palsy or combined low median and ulnar palsies.

This study is the first to provide a complete description of tension at all forefinger tendons during the production of functional static fingertip forces in the non-paretic and parietic forefinger. Knowing tendon tensions is clinically important as it, for example, may help identify tendons at risk of repetitive motion disorders (Rempel et al., 1992; Schuind et al., 1992; Dennerlein et al., 1998). However, in vivo measurements of tendon tensions (Table 3) are limited to flexor tendons, and are difficult to compare

Table 3  
Comparison of the ratio of tendon tension to fingertip force among two in vivo studies and this study<sup>a</sup>

Source	FP	FS	EI	EC	LUM	DI	PI
This study, <i>n</i> = 11 (in situ)	2.8 (0.98)	1.33 (1.04)	0.33 (0.45)	0.73 (0.85)	0.11 (0.19)	2.22 (0.67)	0.0 (0)
Dennerlein et al. (1998), <i>n</i> = 5 (in vivo)		2.4 (0.6)					
Schuind et al. (1992), <i>n</i> = 5 (in vivo)	7.9 (6.3)	1.7 (1.5)					

<sup>a</sup>These data represent the only available direct measurements of tendon tension during static fingertip force production. Mean (SD). All data for this study are also shown in Fig. 5. Note that differences in the direction of fingertip force and forefinger posture preclude accurate comparisons across studies.

because instructions to participants, fingertip force directions and finger posture are not standardized across studies. Because all tendon tensions in all cadaver specimens are known in this study, we see the ratios of tendon tension to fingertip force magnitude of FP and FS (Fig. 5B and Table 3) are numerically lower than those reported in vivo (likely due to differences in the nature of the task), and that the mean ratios for FP and EI were lower for low ulnar palsy than the non-paretic case ( $p < 0.05$ ; Fig. 5B). Note also that ratios for DI are comparable to those of the extrinsic flexors for the non-paretic and low radial palsy cases, further underscoring the importance of DI to palmar force production.

Applying optimal combinations of tendon tension to cadaveric forefingers in simulated low radial palsy shows the absence of extensor muscles suffices to weaken fingertip force. The activity of EI and EC (and the inactivity of PI, Fig. 5) for palmar force in the non-paretic case agrees with EMG recordings of sub-maximal (Close and Kidd, 1969; Long et al., 1970; Valero-Cuevas, 2000) and maximal (Valero-Cuevas et al., 1998) forces. These coordination patterns also agree with predictions of a biomechanical model of the forefinger (Valero-Cuevas et al., 1998; Valero-Cuevas, 2000), supporting the notion that the coordination of finger musculature is strongly influenced by mechanical principles. Simulated low ulnar palsy is seen to severely weaken fingertip force and reduce the ability to direct that force. Accurately directing fingertip force is necessary to grasp small or slippery objects (Murray et al., 1994). Thus, loss of force direction accuracy may be an important, and previously unidentified, contributor to loss of dexterity in fine manipulation — even in the absence of the claw deformity associated with low ulnar palsy.

### Acknowledgements

The Rehabilitation Research and Development Service of the Department of Veterans Affairs supported this work (project number B898). The authors wish to thank Dr. Scott Yerby for the use of his laboratory space; Mr. James Anderson, Mr. Eric Topp and Ms. Larisa Migachov for their aid in constructing the experimental

apparatus; Dr. Felix E. Zajac and Ms. Elise M. Johanson for their insightful comments during the development of this project; and Nathan R. Wilson, MEng for his aid in creating the interactive visualization of data on the Elsevier web page.

### References

- An, K.N., Chao, E.Y., Cooney, W.P., Linscheid, R.L., 1979. Normative model of the human hand for biomechanical analysis. *Journal of Biomechanics* 12, 775–788.
- An, K.N., Chao, E.Y., Cooney, W.P., Linscheid, R.L., 1985. Forces in the normal and abnormal hand. *Journal of Orthopedic Research* 3, 202–211.
- An, K.N., Ueba, Y., Chao, W.P., Cooney, E.Y., Linscheid, R.L., 1983. Tendon excursion and moment arm of index finger muscles. *Journal of Biomechanics* 16, 419–425.
- Brand, P., Hollister, A., 1993. *Clinical Mechanics of the Hand*, 2nd Edition. Mosby-Year Book, Inc., St. Louis.
- Brand, P.W., 1990. Tendons transfer reconstruction for radial, ulnar, median, and combination paralyses: principles and techniques. In: (McCarthy, J. Ed.), *Plastic Surgery*, vol. 8, 1st Edition. W.B. Saunders Company, Philadelphia (Chapter 114).
- Bunnell, S., 1948. *Surgery of the Hand*. J.B. Lippincott Co, Philadelphia.
- Chvátal, V., 1983. *Linear Programming*. W.H. Freeman and Company, New York.
- Close, J.R., Kidd, C.C., 1969. The functions of the muscles of the thumb, the index, and long fingers. Synchronous recording of motions and action potentials of muscles. *Journal of Bone and Joint Surgery (American)* 51, 1601–1620.
- Dennerlein, J.T., Diao, E., Mote Jr., C.D., Rempel, D.M., 1998. Tensions of the flexor digitorum superficialis are higher than a current model predicts. *Journal of Biomechanics* 31, 295–301.
- Garcia-Elias, M., An, K.N., Berglund, L., Linscheid, R.L., Cooney, W.P., Chao, E.Y., 1991. Extensor mechanism of the fingers: I. A quantitative geometric study. *Journal of Hand Surgery (American)* 16, 1130–1140.
- Greenwald, D., Shumway, S., Allen, C., Mass, D., 1994. Dynamic analysis of profundus tendon function. *Journal of Hand Surgery (American)* 19, 626–635.
- Hamman, J., Ali, A., Phillips, C., Cunningham, B., Mass, D.P., 1997. A biomechanical study of the flexor digitorum superficialis: effects of digital pulley excision and loss of the flexor digitorum profundus. *Journal of Hand Surgery (American)* 22, 328–335.
- Hume, E.L., Hutchinson, D.T., Jaeger, S.A., Hunter, J.M., 1991. Biomechanics of pulley reconstruction. *Journal of Hand Surgery (American)* 16, 722–730.
- Hurlbut, P.T., Adams, B.D., 1995. Analysis of finger extensor mechanism strains. *Journal of Hand Surgery (American)* 20, 832–840.

- Ikebuchi, Y., Murakami, T., Ohtsuka, A., 1988. The interosseous and lumbrical muscles in the human hand, with special reference to the insertions of the interosseous muscles. *Acta Medica Okayama* 42, 327–334.
- Jacobson, M.D., Raab, R., Fazeli, B.M., Abrams, R.A., Botte, M.J., Lieber, R.L., 1992. Architectural design of the human intrinsic hand muscles. *Journal of Hand Surgery (American)* 17, 804–809.
- Lieber, R.L., Jacobson, M.D., Fazeli, B.M., Abrams, R.A., Botte, M.J., 1992. Architecture of selected muscles of the forearm: anatomy and implications for tendon transfer. *Journal of Hand Surgery (American)* 17, 787–798.
- Long, C., Conrad, P.W., Hall, E.A., Furler, S.L., 1970. Intrinsic-extrinsic muscle control of the hand in power grip and precision handling. An electromyographic study. *Journal of Bone and Joint Surgery (American)* 52, 853–867.
- Mathiowetz, V., Kashman, N., Volland, G., Weber, K., Dowe, M., Rogers, S., 1985. Grip and pinch strength: normative data for adults. *Archives of Physical Medicine and Rehabilitation* 66, 69–74.
- Mick, J.E., Reswick, J.B., Hager, D.L., 1978. The mechanism of the intrinsic-minus finger: a biomechanical study. *Journal of Hand Surgery (American)* 3, 333–341.
- Murray, R.M., Li, Z., Sastry, S.S., 1994. *A Mathematical Introduction to Robotic Manipulation*. CRC Press, Boca Raton, FL.
- Nishida, J., Amadio, P.C., Bettinger, P.C., An, K.N., 1998. Flexor tendon-pulley interaction after pulley reconstruction: a biomechanical study in a human model in vitro. *Journal of Hand Surgery (American)* 23, 665–672.
- Rempel, D.M., Harrison, R.J., Barnhart, S., 1992. Work-related cumulative trauma disorders of the upper extremity. *Journal of the American Medical Association* 267, 838–842.
- Rispler, D., Greenwald, D., Shumway, S., Allan, C., Mass, D., 1996. Efficiency of the flexor tendon pulley system in human cadaver hands. *Journal of Hand Surgery (American)* 21, 444–450.
- Schuind, F., Garcia-Elias, M., Cooney, W.P.d., An, K.N., 1992. Flexor tendon forces: in vivo measurements. *Journal of Hand Surgery (American)* 17, 291–298.
- Spoor, C.W., 1983. Balancing a force on the fingertip of a two dimensional finger model without intrinsic muscles. *Journal of Biomechanics* 16, 497–504.
- Tubiana, R., 1981. In: Tubiana, R. (Ed.), *The Hand*. Saunders, Philadelphia.
- Valero-Cuevas, F.J., Zajac, F.E., Burgar, C.G., 1998. Large index-fingertip forces are produced by subject-independent patterns of muscle excitation. *Journal of Biomechanics* 31, 693–703.
- Valero-Cuevas, F.J., 2000. Predictive modulation of muscle coordination pattern magnitude scales fingertip force magnitude over the voluntary range. *Journal of Neurophysiology* 83, 1469–1479.
- Weightman, B., Amis, A., 1982. Finger joint force predictions related to design of joint replacements. *Journal of Biomedical Engineering* 4, 197–205.
- Yoshikawa, T., 1990. *Foundations of Robotics: Analysis and Control*. The MIT Press, Cambridge.
- Zancolli, E., Cozzi, E.P., 1992. *Atlas of Surgical Anatomy of the Hand*. Churchill Livingstone, New York.

Erratum

Quantification of fingertip force reduction in the forefinger following simulated paralysis of extensor and intrinsic muscles

Francisco J. Valero-Cuevas, Joseph D. Towles, Vincent R. Hentz

---

The Publisher regrets that in the above article published in *Journal of Biomechanics* 33, 1601–1609 (2000), on p. 1605, an incorrect link to the journal's webpage was published.

The correct link is reproduced below and will allow access to supplementary material for the above article:  
<http://www.mae.cornell.edu/valero/JBiomech/>